

# Laser-annealing of thin semiconductor films

J.Boneberg, J.Nedelcu, E.Bucher, P.Leiderer  
Universität Konstanz, 78464 Konstanz, Germany

## ABSTRACT

Optical reflectivity and transmissivity measurements have been used to investigate the dynamics of melting and recrystallisation of thin films of Si and Ge after laser-annealing with a ns Nd:YAG-laser pulse. We report on temperature dependent changes of the reflectivity of the liquid phase above and below the melting point and on various nucleation and solidification scenarios in thin films, depending on the energy density of the annealing laser.

## 1. INTRODUCTION

The interaction of semiconductor surfaces with intense laser radiation is a long-standing topic, which has led to a number of interesting phenomena. In particular, the melting and subsequent resolidification of a thin surface layer on bulk semiconductors has been investigated in detail.<sup>1,2</sup> One aim of this "laser annealing" procedure was to remove defects in the crystal structure of the semiconductor introduced, e.g., by ion implantation. Apart from this application, the processes occurring during the rapid temperature quench of a thin liquid layer are interesting also from the fundamental point of view, for example with respect to the processes which limit the velocity of crystal growth.

In this work we report on laser-induced melting and solidification of thin films of Si and Ge, investigated by optical reflection and transmission measurements with nanosecond time resolution. The intention was to study the liquid phase at temperatures above the melting point  $T_m$ , as well as the dynamics of nucleation of crystallites from the melt and the formation of metastable phases, such as amorphous Si. Laser annealing experiments allow to achieve very high cooling rates ( $dT/dt \geq 10^{10}$  K/s) and large supercooling of the liquid phase down to temperatures of the order of  $T_m/2$ , and thus make experimental ranges accessible which by other means are difficult to reach.<sup>3</sup>

Optical measurements appear very suitable for these studies, because the reflection and transmission properties differ strongly between the respective phases, and in addition in each phase also depend on the temperature. Starting from crystalline Si at 300 K, e.g., the reflection coefficient  $R$  (at  $\lambda = 632.8$  nm and perpendicular incidence) increases from 36% to a value of 42% at the melting temperature  $T_m = 1680$  K. Upon the appearance of the liquid phase, which is metallic,  $R$  jumps up to 70%, and then slowly decreases again as the temperature is raised further.<sup>4</sup> For thin films additional temperature dependences of  $R$  appear as a result of the interference of light reflected from the film surface and the interface between film and substrate.

## 2. LIQUID PHASE

In the experiments to be described here the semiconductor surfaces were irradiated with the light of a pulsed Nd:YAG laser operating in the frequency doubled mode ( $\lambda = 532 \text{ nm}$ ) at a pulse width of 5 ns and energies up to 100 mJ per pulse.

We present first some results for the surface of bulk semiconductors. Fig. 1a shows a snapshot of a circular patch of liquid Si, molten by the Nd:YAG laser beam, taken at a time  $t = 30 \text{ ns}$  after the laser pulse. The liquid phase appears bright here, due to its higher reflectivity. In order to obtain this picture, part of the incident Nd:YAG beam was split off, passed through a delay line and shifted in frequency by means of stimulated Raman scattering (see Fig. 1b). This light was then guided at the sample surface, where it was reflected and, after passing through an color filter which rejected the stray light of the high intensity primary beam, recorded by a video camera. The time evolution of the molten spot can in this way be monitored by varying the delay line of the probe pulse for successive pulses. The temporal resolution of the snapshot, given by the length of the probe pulse, was 5 ns.

*Fig. 1a: Ns-photograph of a laser-molten Si layer on bulk Si. The picture was taken 30 ns after the primary pulse.*

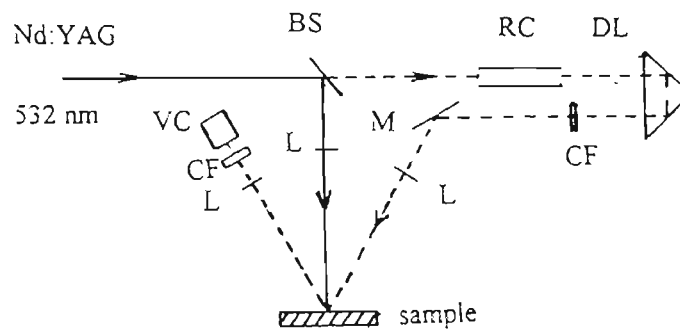
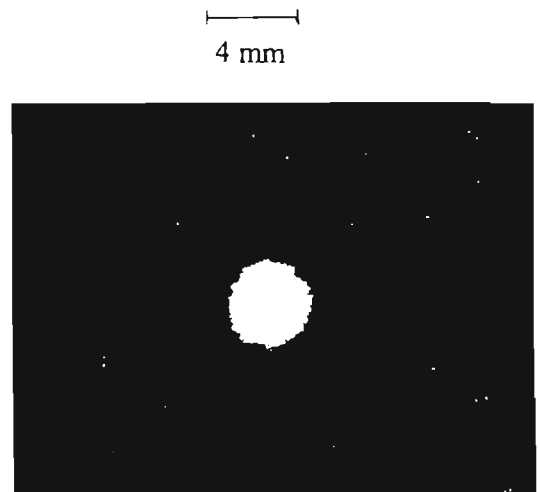


*Fig. 1b: Experimental set-up for ns photography*

BS: beamsplitter	RC: Raman cell	DL: delay line
VC: video camera	M: mirror	L: lens
		CF: color filter

Since in the following we are mainly interested in the processes at the centre of the primary beam, we show results obtained with a slightly modified set-up (Fig.2). The probe beam is now supplied by a low power cw-laser, focussed to a diameter of  $10\ \mu\text{m}$ , much smaller than the size of the primary beam of typically  $0.5\ \text{mm}$ . The specularly reflected light at the wavelength  $633\ \text{nm}$  was detected by a pin diode (risetime  $< 1\ \text{ns}$ ) and registered by a fast digital storage oscilloscope (HP54111D). In order to obtain as much information as possible from each laser pulse, we used in general several probe lasers at various wavelengths simultaneously, all focussed to the same spot and diameter. Moreover in the case of thin film samples we measured in addition to the reflectivity of the surface (henceforth designated as  $R_s$ ) also the reflectivity of the film-substrate interface  $R_i$ , and the transmissivity of the sample. Interference filters in front of the pin diodes suppressed contributions of the Nd:YAG light to the measured signals.

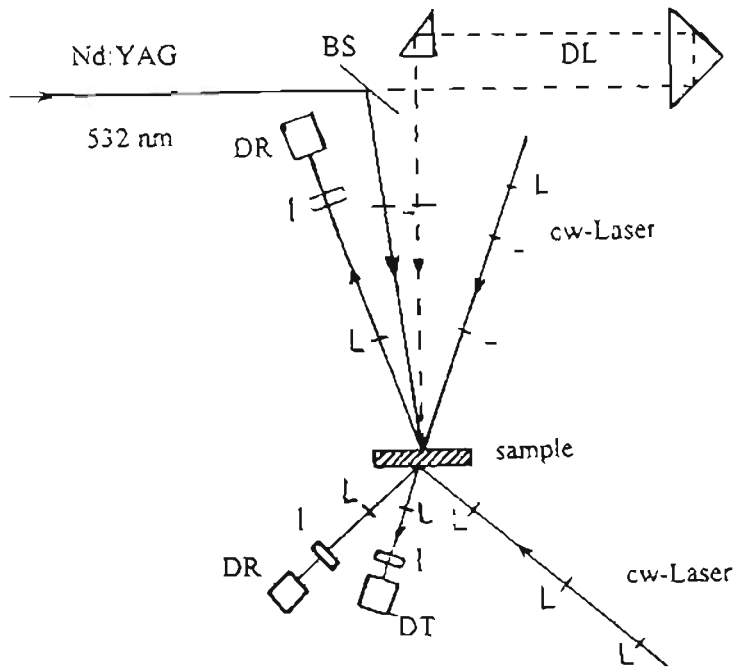


Fig.2: Experimental set-up for the time-resolved reflectivity and transmissivity experiments

BS: beam splitter      DT: diode for transmission      L: lens  
 I: interference filter      DR: diode for reflection      DL: delay line

## 2.1 SINGLE PULSE EXPERIMENTS

Fig.3 shows the time-resolved reflectivity  $R_s$  for the wavelength  $633\ \text{nm}$  during laser-annealing of bulk Si and Ge with different energy densities of the pulse laser. Upon melting of the surface a drastic increase of the reflectivity is observed, indicating the change from the semiconducting solid to the

metallic liquid phase. As long as a liquid layer with a thickness larger than approximately two times the absorption length ( $d_{ab} \approx 10 \text{ nm}$ )<sup>5</sup> exists at the surface the reflectivity remains constant at the high metallic value. After solidification  $R$  decreases on a  $\mu\text{s}$ -timescale towards the starting point as the temperature drops.

Using such measurements we can obtain the melting time (the duration of the high reflectivity phase) for different energy densities (Fig.4). This measurement can be compared with the results of heat flow calculations based on the finite difference method.<sup>6</sup> Fig.4 shows excellent agreement between our calculation (solid line in Fig.4) and experiment as long as the energy density of the laser pulse is below  $1.2 \text{ J/cm}^2$ . At higher energy densities the calculation leads to systematically smaller melting times (see below). This deviation at higher energy densities suggests that there may be a temperature effect on the reflectivity properties of the liquid. We have therefore examined the temperature dependence of  $R_S$  using the double pulse experiment, discussed in the following chapter.

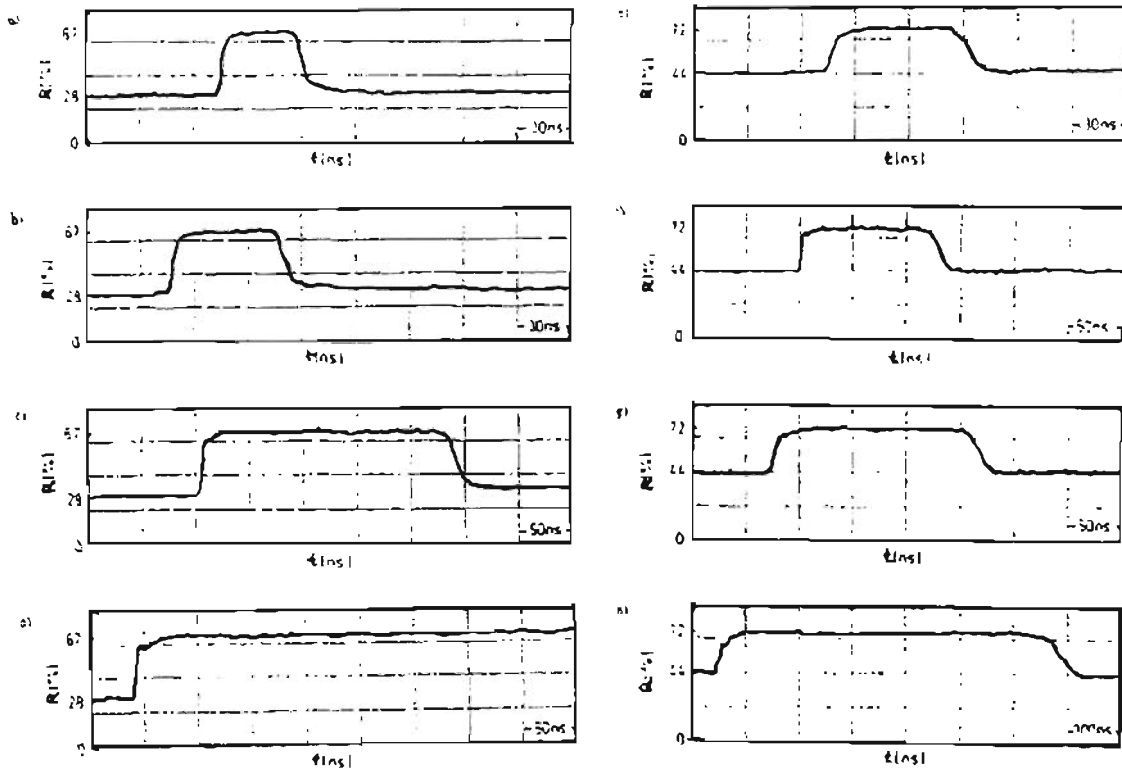


Fig.3: Time-resolved reflectivity  $R_S$  ( $\lambda = 633 \text{ nm}$ ) at different energy densities:  
 target: Si a)  $0.9 \text{ J/cm}^2$  b)  $1.0 \text{ J/cm}^2$  c)  $2.0 \text{ J/cm}^2$  d)  $2.3 \text{ J/cm}^2$   
 Ge e)  $0.6 \text{ J/cm}^2$  f)  $0.75 \text{ J/cm}^2$  g)  $0.9 \text{ J/cm}^2$  h)  $1.3 \text{ J/cm}^2$

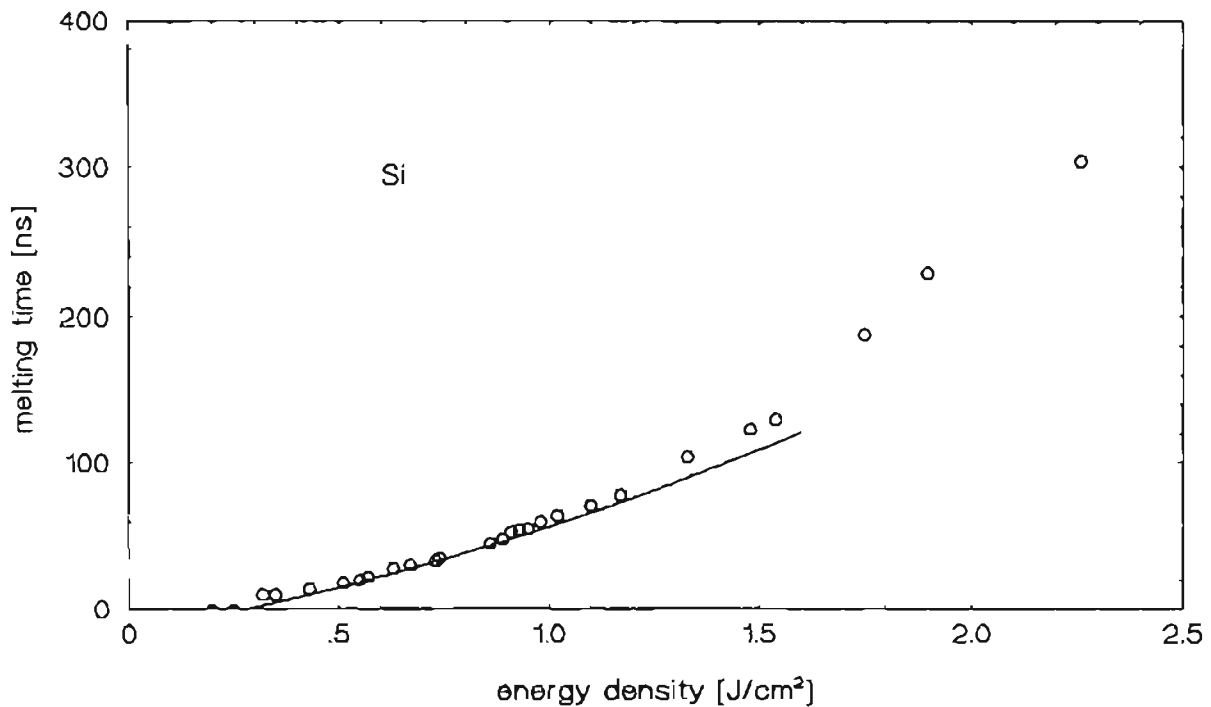


Fig.4: Melting time of Si as function of the energy density of the annealing laser  
 solid line: calculated      circles: measured

## 2.2 DOUBLE PULSE EXPERIMENT

In principle, information about the laser-induced change of the surface temperature and reflectivity in the liquid state can be obtained from single pulse experiments. However, the double pulse measurements described here are interpreted more readily: The leading pulse generates a molten layer thick compared to the penetration depth of the laser light, so that the second pulse - which is the one to be analyzed in detail - is absorbed under well-defined conditions. Moreover, the effects due to heating the liquid surface are relatively subtle and thus in a single pulse experiment are easily obscured by the huge change in the reflectivity upon melting. By contrast, in a double pulse experiment these two processes are well separated, since the second pulse arrives with a delay of several ten ns.

In the examples given below for Si the energy density of the first pulse was held fixed at  $E_1 = 1.0 \text{ J/cm}^2$ , whereas the energy density of the delayed pulse was varied. In Fig. 5a-d four reflectivity curves  $R_S$  are plotted for  $E_2 = 0, 0.5, 1.4, \text{ and } 1.8 \text{ J/cm}^2$ , respectively. Fig. 5a, which represents the

effect of laser heating by the first pulse alone, shows that at the given energy density a molten layer is created which exists for 55 ns, in good agreement with previous work<sup>2</sup>. In the trace of Fig.5b, the reflectivity appears not to be affected within the experimental resolution as the delayed pulse (whose position is marked by an arrow) hits the surface. Nevertheless, the additional energy input due to the second pulse manifests itself in an increased lifetime of the high reflectivity liquid phase, 125 ns in this case. As the energy of the second pulse is further increased, however, the heating of the liquid surface leads to a clearly discernible dip in the reflectivity (e.g.  $\Delta R = 3.4\%$  at  $E_2 = 1.4 \text{ J/cm}^2$  in Fig.5c). This dip becomes even more pronounced at higher energies, reaching  $\Delta R = 9\%$  at  $E_2 = 1.8 \text{ J/cm}^2$  (Fig.5d). Similar results have been found for Ge.

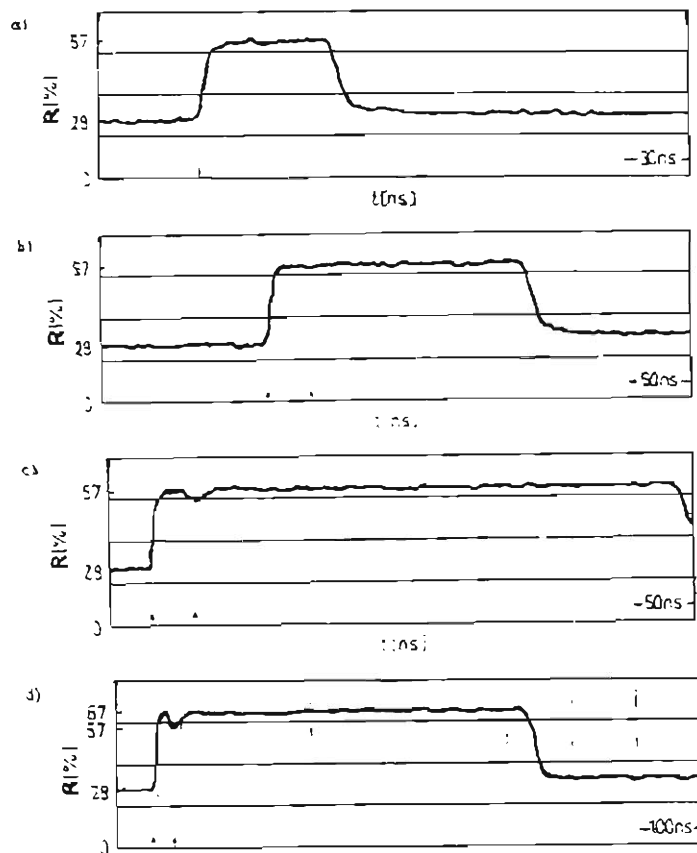


Fig.5: Time-resolved reflectivity  $R_S$  ( $\lambda = 633 \text{ nm}$ ) of Si in double pulse experiments  
 $I_1 = 1.0 \text{ J/cm}^2$  in all cases,  $I_2 = 0.0 \text{ J/cm}^2$  (a),  $0.9 \text{ J/cm}^2$  (b),  $1.5 \text{ J/cm}^2$  (c),  $1.9 \text{ J/cm}^2$  (d)  
 Laser pulses are marked by arrows

Using both the results from the heat diffusion calculation and the energy dependence we can infer the temperature effect on the reflectivity of liquid Si (Fig.6). As it appears Si in the molten state does not behave like a simple Drude metal; the data suggest that the density of free electrons, respectively the plasma frequency, is not constant but increases with temperature (for details see Ref. 7).

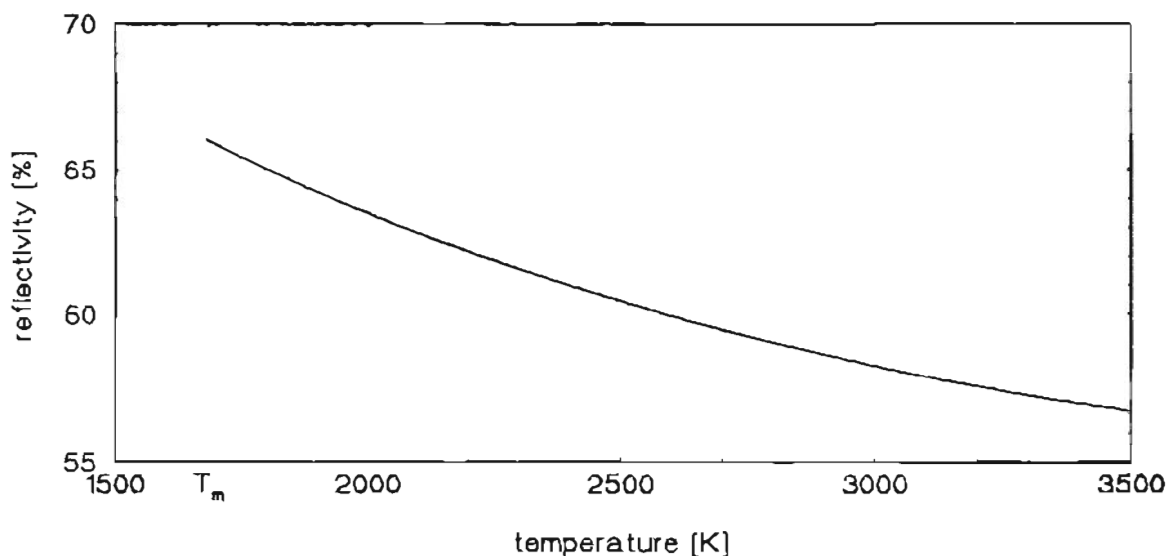


Fig.6: Calculated reflectivity ( $\lambda = 633 \text{ nm}$ ) of liquid Si above the melting point  $T_m$  as a function of temperature

The decrease of the reflectivity with increasing temperature explains the discrepancy between heat flow calculations and measurements (Fig.4): At higher energy densities the temperature of the surface increases considerable, the reflectivity drops and therefore the absorption and the melting time increase.

We want to point out an observation at even higher temperatures which might be interpreted as a metal-insulator transition in liquid Si.<sup>8</sup> In these measurements, which have been made with *thin Si films* (cf. part3), the reflectivity and transmissivity were determined simultaneously at two probe wavelengths 633 nm and 488 nm. While at energy densities discussed so far the reflectivity remained at a high value upon melting (cf. Fig.10), it is observed in Fig.7 that at even higher energy density the reflectivity drops below 10% after a quick increase up to the reflectivity of the molten Si. The transmissivity, on the other hand, which had been zero in the liquid phase for the measurements at lower energy densities, now increases above 90%. Thus the film in this state behaves rather as a transparent dielectric than a liquid metal. This behavior might result from thermal expansion upon heating, and is in line with a metal-insulator transition at sufficiently small electron densities.

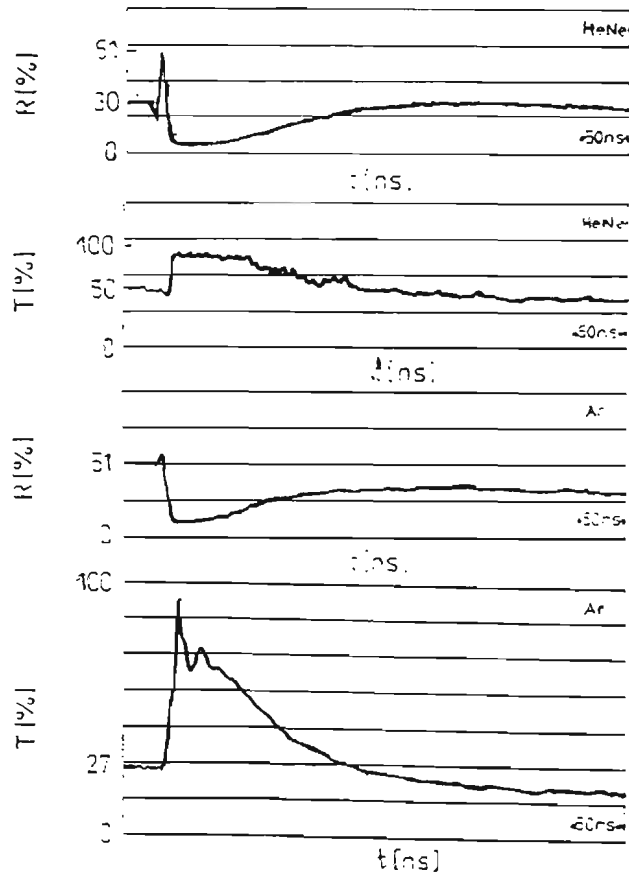


Fig.7: Time-resolved reflectivity and transmissivity ( $\lambda = 633 \text{ nm}$  and  $488 \text{ nm}$ ) of a thin Si-film ( $d = 125 \text{ nm}$ ) on a quartz glass substrate at an energy density of  $400 \text{ mJ/cm}^2$

### 3. SOLIDIFICATION SCENARIOS ON THIN SI-FILMS

The samples used here were polycrystalline Si films with a thickness of 125 nm on 1 mm quartz glass substrates. The experimental results can be divided into three regimes, depending on the energy density of the annealing-laser: 3.1) heating without melting, 3.2) partial melting and 3.3) complete melting of the Si film.

#### 3.1 HEATING OF THE SOLID PHASE

As long as the energy density of the annealing laser pulse is sufficiently low ( $E < E_{thres} = 170 \text{ mJ/cm}^2$ ) the film does not melt. In the experimental curve shown in Fig.8 the energy density of the laser pulse is just below  $E_{thres}$ . The surface reflectivity  $R_s$  decreases from 70% to 30% and the reflectivity



on the substrate side  $R_i$  decreases from 50% to 40% during the laser pulse. Both increase back to the starting value on a time scale of 200 ns. The observed reflectivity changes are due to an interference effect in the thin film and can be interpreted by means of the temperature dependence of the optical constants of crystalline Si.<sup>10,11</sup> Calculations of the reflectivity from thin film optics agree very well with the observed reflectivity changes.

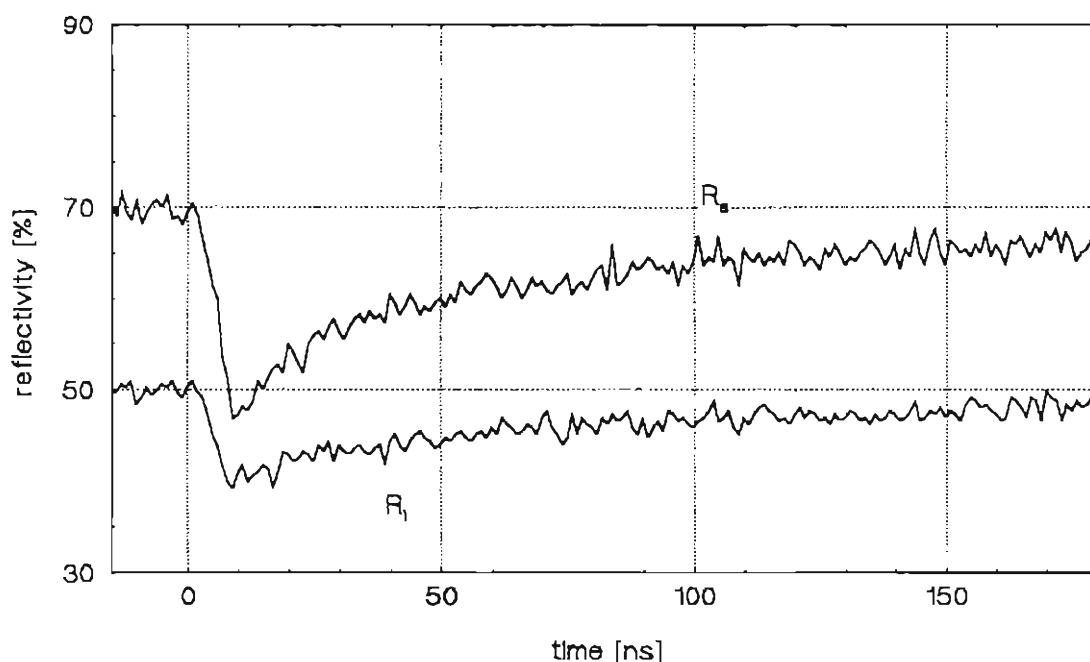


Fig.8: Time-resolved reflectivity ( $R_s$  at 633 nm and  $R_i$  at 488nm) of a thin Si film ( $d = 125$  nm) at an energy density of  $I=160$  mJ/cm<sup>2</sup>, just below the threshold of melting

### 3.2 PARTIAL MELTING OF THE SI-FILM

As the energy density is increased above  $E_{thres}$  a surface layer of the Si-film is melted. The surface reflectivity  $R_s$  (Fig.9) shows first a decrease and then rises to a plateau value during the laser pulse. For several ns  $R_s$  is constant then before it decreases once again. Afterwards  $R_s$  relaxes back to the starting value. This behavior is easily interpreted:  $R_s$  decreases first with increasing temperature as we have seen in 3.1. Upon melting the reflectivity rises to the reflectivity of liquid Si.  $R_s$  is then constant as long as a liquid layer is present at the surface with a thickness  $d_l \geq 2 d_{ab}$ . With further decreasing thickness of the liquid layer  $R_s$  decreases to the reflectivity of the hot solid Si near the melting point as shown in the previous chapter.

The reflectivity of the substrate interface  $R_i$  decreases first as the layer is heated as shown in 3.1. As the boundary liquid-solid approaches the substrate  $R_i$  increases until a maximum value is reached. From the fact that the reflectivity of liquid Si is not reached one can conclude that a thin layer of Si next to the interface was not melted. The solidification proceeds from the unmelted Si layer towards the surface and  $R_i$  approaches the value of hot solid Si at the melting point.

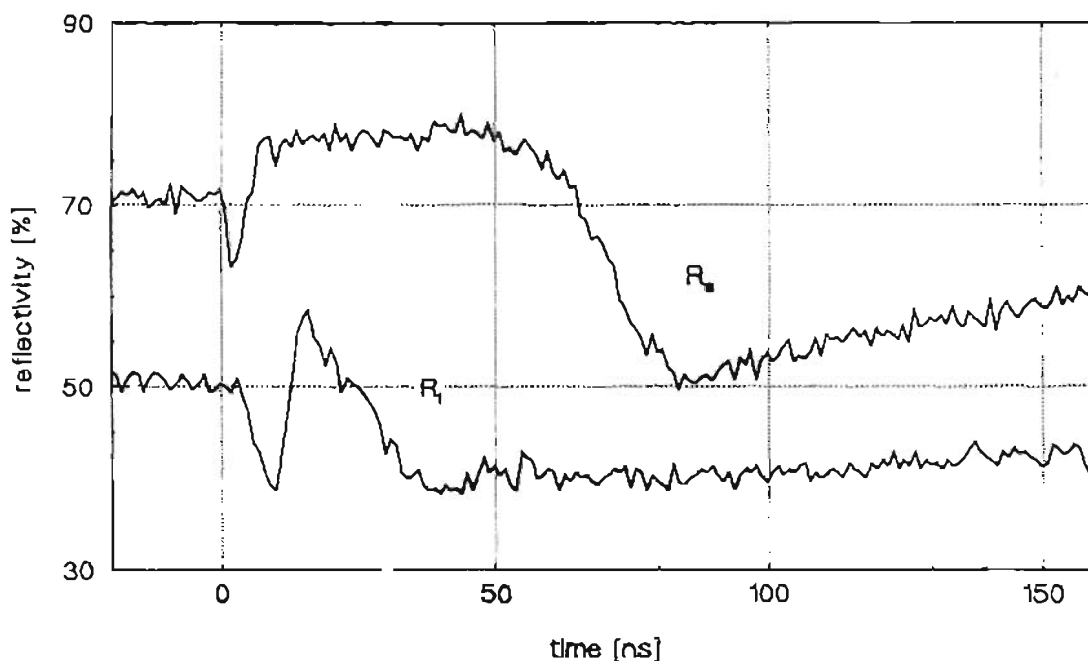


Fig.9: Time-resolved reflectivity ( $R_s$  at 633 nm and  $R_i$  at 488nm) of a thin Si film ( $d = 125$  nm) at an energy density  $I=240$  mJ/cm<sup>2</sup>

### 3.3 COMPLETE MELTING OF THE SI-FILM

Upon complete melting of the Si film the solidification scenario changes from heterogeneous nucleation and solidification starting from the liquid-solid interface, as outlined above, towards homogeneous nucleation in the supercooled liquid. We start the discussion of the homogeneous nucleation phenomena with the highest energy density that we used in this experiment:

Fig.10 shows the reflectivity curves for an energy density 360 mJ/cm<sup>2</sup>. Compared to Fig.9  $R_s(t)$  exhibits an additional very pronounced feature. Between the plateau that we related to the liquid Si surface and the region where the solid Si cools down there exists a second plateau with a reflectivity below the value of liquid Si. Moreover the  $R_i$  curve now displays a region (between  $t = 20$  and 70 ns) where the reflectivity is nearly constant.

Stiffler and Thompson<sup>3</sup> proposed the following model for this behavior: During the first plateau the liquid Si cools down to a temperature several hundred degrees below the melting point. Homogeneous nucleation throughout the film initiates solidification and therefore a decrease in the reflectivity. The latent heat released upon solidification raises the temperature towards the melting point, where further solidification is stopped. The layer consists now of solid Si in a liquid matrix and has a reflectivity which is smaller than the reflectivity of liquid Si alone. The complete solidification proceeds then from the substrate towards the surface.  $R_S$  therefore shows a second plateau, until the complete solidification reaches the surface layer.

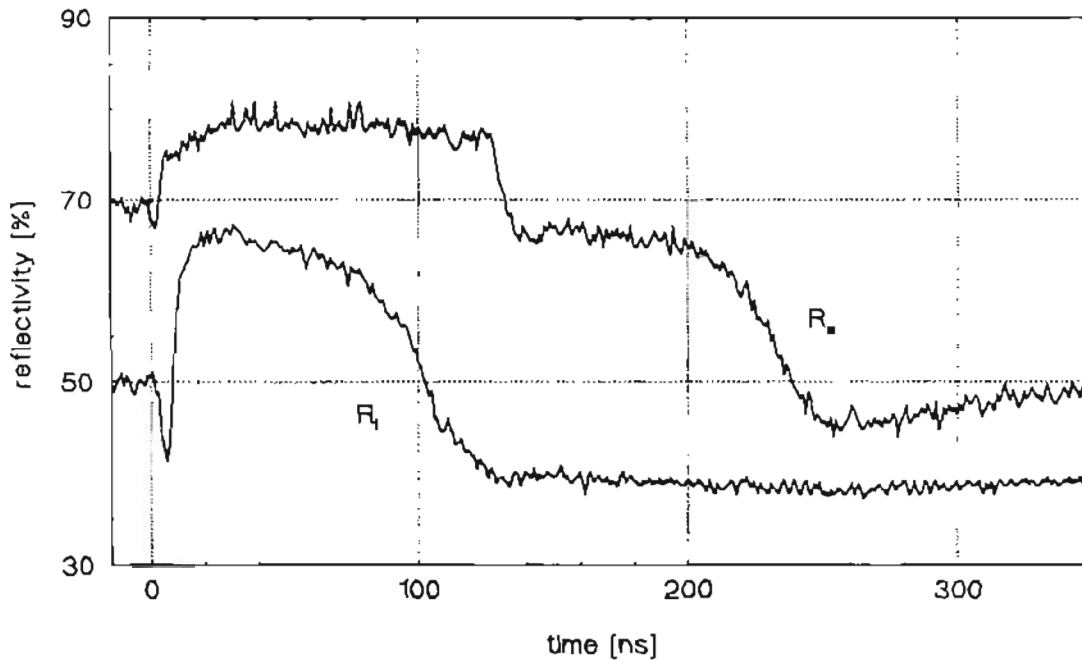


Fig.10: Time-resolved reflectivity ( $R_S$  at 633 nm and  $R_i$  at 488nm) on a thin Si film ( $d = 125$  nm) at the energy density  $I=360$  mJ/cm<sup>2</sup>

This model of Stiffler and Thompson is in good accord with the  $R_S$  curve in Fig.10. Yet additional information is obtained from our simultaneous measurement of  $R_i$ . The steep decrease of  $R_i$  occurs about 25 ns earlier than the decrease of  $R_S$ . One can conclude that the homogeneous nucleation and solidification proceeds from the substrate towards the surface. Furthermore there is no second plateau in  $R_i$ , indicating that solidification at the substrate side is completed in one step. From the result that the solidification at the surface is a two-step process we get the information that during the partial solidification a gradient in the solidified volume exists across the layer.

We will now return to smaller energy densities until we reach  $E_{compl}$ , where the thin film is just melted completely. In terms of supercooling this procedure means that we increase the supercooling now: The highest quench rates - and therefore supercoolings - are achievable at the highest heat fluxes into the substrate. As the heat flux into the substrate decreases with time, caused by the decrease of the temperature gradient, somewhat surprisingly the smallest energy density ( $E_{compl}$ ) yields the maximum supercooling. A calculation based on heat flux considerations yields values well beyond 500 K for the maximum supercooling achieved in our experiments.

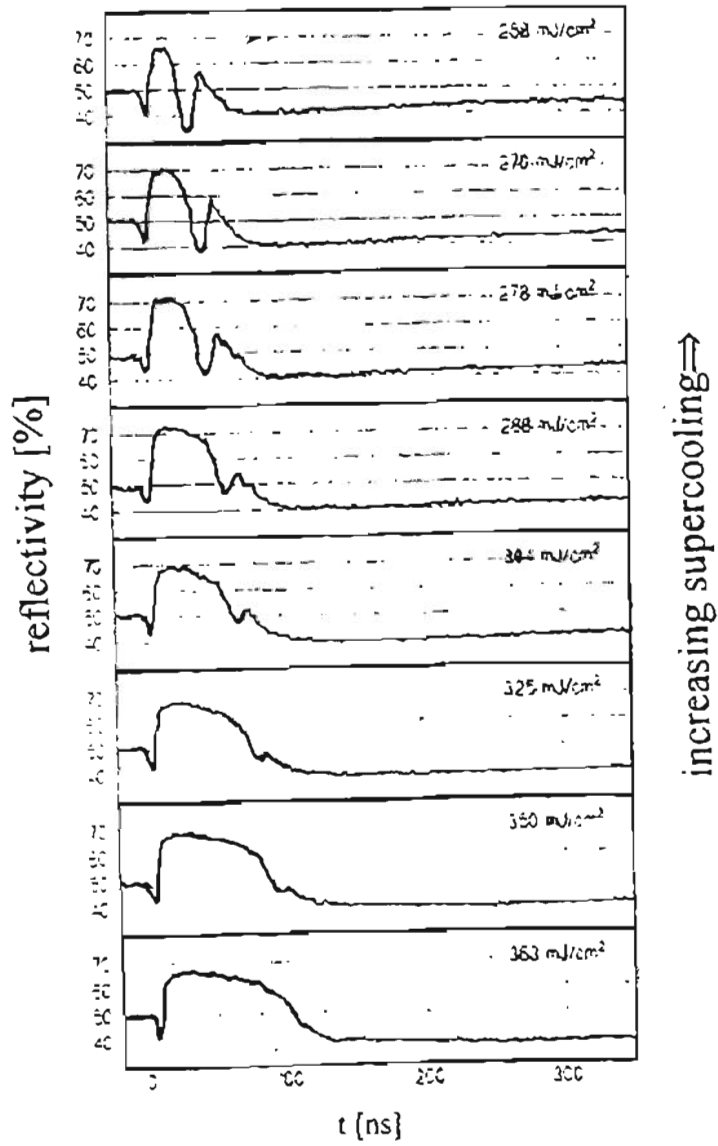


Fig. 11: Time-resolved reflectivity ( $R_i$  at 488nm) of a thin Si-film ( $d = 125 \text{ nm}$ ). Decreasing energy density corresponds to increasing supercooling

From thermodynamical reasons at high supercooling the nucleation of crystalline as well as the nucleation of amorphous Si is possible.<sup>3</sup> Upon proceeding to larger undercooling an additional peak arises in the  $R_i$  curves (Fig. 11). In our interpretation this peak is connected with a transient formation of amorphous Si. As the temperature of the Si layer is raised above the melting point of amorphous Si  $T_{m,a}$  (1435 K)<sup>3</sup> amorphous regions are melted and  $R_i$  increases. Upon crystallisation  $R_i$  decreases once again. The optical properties of the Si layer at room temperature after the annealing process does not show any change which could be attributed to the *permanent* formation of amorphous Si. This observation is in agreement with the measurements of Sameshima and Usui<sup>12</sup> who found permanent amorphisation only at film thicknesses below 18 nm.

The  $R_s$  curves show the effect of remelting as well, but in somewhat modified form: The remelting does not increase continuously with the supercooling. We suppose that the latent heat released upon nucleation on the substrate side alters the nucleation on the surface side, which always takes place some tens of ns later.

Regarding the temperature dependence of the reflectivity the measurements on thin liquid Si films confirm the observation of part 2: At the end of the laser pulse the temperature of the liquid reaches its maximum. As the temperature decreases the reflectivity increases (cf.  $R_s$  in Fig. 10 between  $t = 5$  and 35 ns). During the following undercooling no further increase of  $R_s$  can be observed (cf.  $R_s$  in Fig. 10 between  $t = 35$  and 120 ns). On the contrary  $R_s$  decreases again in contrast to the expectations of a simple Drude-metal (a similar feature can be found in the conductivity of liquid Si<sup>9</sup>). This behavior can be understood if one assumes (as we already did in part 2 and in Ref. 7) that, apart from a temperature dependent change of the collision frequency, the density of the free electrons in the melt is temperature dependent as well: The density of free electrons is decreasing with decreasing temperature. This change of the electron density becomes the dominant effect at temperatures below the melting temperature. As a result  $R(T)$  has a maximum at temperatures around the melting point.

#### 4. SUMMARY

In summary we have shown that liquid Si and Ge show temperature dependent optical properties, which have to be considered in model calculations of the heat balance in laser-annealing. The temperature dependence of the optical properties is not given by a simple Drude behavior but has an additional contribution of a the temperature dependent change of the electron density. At high temperatures we observe an optical behavior, which suggests a metal - insulator transition in the liquid.

Concerning the solidification phenomena we have shown that the simultaneous measurement of the reflectivity from the surface and the substrate side gives comprehensive information about nucleation and solidification in thin films. Regions of heterogeneous and homogeneous nucleation as well as transient amorphisation and the influence of the temperature gradient across the film could be resolved.

## 5.ACKNOWLEDGEMENTS

We would like to thank M.O.Thompson for a day of stimulating discussion and for providing a preprint of his recent work prior to publication. This work was supported by Zentrum II für Energieforschung at the University of Konstanz.

## 6.REFERENCES

1. J.M.Poate Laser Annealing of Semiconductors, Academic Press, New York, 1982
2. D.H.Auston, J.A.Golovchenko, A.L.Simons, R.E.Slusher, P.R.Smith, C.M.Surko, and T.N.C.Venkatesan, Dynamics of Laser Annealing, Laser Solid Interactions and Laser Processing, AIP, New York, 1979
3. S.R.Stiffler, M.O.Thompson, P.S.Peercy, "Supercooling and Nucleation of Silicon after Laser Melting", *Phys.Rev.Lett.*, vol.60,24, pp. 2519-2522, 1988
4. M.O.Lampert, J.M.Koebel, P.Siffert, "Temperature dependence of the reflectance of solid and liquid silicon", *J.Appl.Phys.*, vol.52,8, pp. 4975-4976, 1981
5. G.E.Jellison, Jr. and D.H.Lowndes, "Measurements of the Optical Properties of Liquid Silicon and Germanium Using Nanosecond Time-Resolved Ellipsometry", *Appl.Phys.Lett.*, vol.51,5, pp. 352-354, 1987
6. P.Baeri, S.U.Campisano, G.Foti, and E.Rimini, "A Melting Model for Pulsing-Laser Annealing of Implanted Semiconductors", *Appl.Phys.*, vol 50,2, pp. 788-797, 1979
7. J.Boneberg, O.Yavas, B.Mierswa, P.Leiderer, "Optical Reflectivity of Si above the Melting Point", *phys.stat.sol.(b)*, vol.174, pp.295-300, 1992
8. V.A.Batanov, F.V.Bunkin, A.M.Prokhorov, V.B.Fedorov, "Evaporation of metallic targets caused by intense optical radiation", *Soviet Physics JETP*, vol.36,2, pp.311-322, 1973
9. M.J.Uttormark, M.O.Thompson, S.R.Stiffler, P.S.Peercy, "Conductance of Undercooled Liquid Silicon", unpublished
10. K.Murakami, K.Takita, K.Masuda, "Measurement of Lattice Temperature during Pulsed-Laser Annealing by Time-Dependent Optical Reflectivity", *Jap.J.Appl.Phys.*, vol.20,12, pp.L867-870, 1981
11. G.E.Jellison, Jr. and F.A.Modine, "Optical absorption of silicon between 1.6 and 4.6 eV at elevated temperatures", *Appl.Phys.Lett.*, vol.41,2, pp.180-182, 1982
12. T.Sameshima, S.Usui, "Pulsed laser-induced amorphization of silicon films", *J.Appl.Phys.*, vol.70,3, pp.1281-1289, 1991